

# DYNAMIC CRUSHING OF 2D CELLULAR METALS: MICROSTRUCTURE EFFECTS AND RATE-SENSITIVITY MECHANISMS\*

Jilin Yu\*\* Zhijun Zheng

(CAS Key Laboratory of Mechanical Behavior and Design of Materials,  
University of Science and Technology of China, Hefei 230027, China)

**ABSTRACT** The dynamic response of cellular metals has been extensively investigated due to their excellent properties as impact energy absorbers and blast protectors. In the past years, our group focused on characterizing the dynamic behavior of 2D cellular metals and achieved much understanding of the microstructural effects on the dynamic mechanical properties and the possible mechanisms governing the rate sensitivity of cellular metals. Three types of microstructural randomness and imperfections were employed in the basic topology model of a regular hexagonal honeycomb. Their influences on deformation mode and plateau stress were studied by finite element method using the ABAQUS/Explicit code. The results show that there are three macroscopic deformation modes occurring when a honeycomb is compressed under different impact velocities. Microstructural randomness and imperfections may strongly affect the energy absorption capacity. The influences of the inertia and the properties of cell-wall material on the rate sensitivity of Voronoi honeycombs were explored through numerical 'tests'. The density of cell-wall material was artificially changed to study the influence of inertia, which was found to be the dominant factor in the dynamic crushing of Voronoi honeycombs. The effects of strain hardening and strain-rate hardening of cell-wall materials were examined and found to have minor influence on plateau stress, which cannot explain the strong rate dependence observed in some metal foams.

**KEY WORDS** cellular metals, Voronoi honeycomb, finite element analysis, inertia, strain-rate effect

## I. INTRODUCTION

The dynamic response of cellular metals has been extensively investigated due to their excellent properties as impact energy absorbers and blast protectors. The macroscopic crushing behavior of cellular metals is closely related to their microstructure, especially the randomness and imperfections, so mesoscopic finite element models have been developed to explore its influence. Rate sensitivity of cellular metals has also attracted considerable research interest, but some conflicting experimental results of the rate effect on their deformation behavior exist in the literature<sup>[1,2]</sup>. In the past years, our group focused on characterizing the dynamic behavior of 2D cellular metals and achieved much understanding of the microstructural effects on the dynamic mechanical properties<sup>[3-5]</sup> and the possible mechanisms governing the rate sensitivity of cellular metals<sup>[1,6-8]</sup>. A review on this topic is presented in this paper.

Much work has shown that the mechanical properties of cellular materials are affected by the microstructural parameters, such as relative density, cell size and cell morphology<sup>[3]</sup>. Years ago, researchers focused on investigating the influence of the microstructural parameters on the static crushing behavior of cellular materials<sup>[9]</sup>. Recently, the influences of microstructural randomness and imperfections on the dynamic crushing behavior of cellular materials have been extensively investigated. The cell irregularity<sup>[3]</sup>, randomly distributed solid inclusions<sup>[4,10]</sup>, linearly arranged

---

\* The work reported herein is supported by the National Natural Science Foundation of China (Projects Nos. 90916026, 11002140 and 90205003)

\*\* Corresponding author. Email address: jlyu@ustc.edu.cn.

inclusions<sup>[11]</sup>, randomly removing cell-walls<sup>[5]</sup>, and micro-topology<sup>[12,13]</sup> have been employed to investigate their influences on the dynamic response of honeycombs under impact. The coupling effect of the irregular cell shapes and non-uniform cell wall thickness was also investigated<sup>[14]</sup>.

The rate sensitivity of cellular materials may come from various sources, such as the effects of intrinsic length scale of the material, the rate sensitivity of cell-wall material, the compression and flow of gas in cells, and the microstructural morphology<sup>[1]</sup>. The quantitative work on this topic was less. We artificially changed the inertia and the properties of cell-wall material to investigate their influences on the dynamic response of honeycombs under impact through full cell-based numerical ‘tests’<sup>[1,6-8]</sup>. Besides our work, it was worth to mention the recent work by Ma et al.<sup>[2]</sup>. They compared the cell-based numerical results with those based on a continuum model and a shock wave theory to explore the underlining reason for the argument on the rate dependence of cellular materials.

In this paper, three types of microstructural randomness and imperfections are employed to investigate their influences on dynamic response of 2D cellular materials. Several methods are introduced to explore the possible mechanisms of the rate sensitivity of Voronoi honeycombs.

## II. MESOSCOPIC NUMERICAL MODELS

### 2.1. Honeycomb Models

The basic topology model is a regular hexagonal honeycomb constructed in a rectangle area  $A_0 = L_x \cdot L_y$ , where  $L_x = n_x \cdot 3^{1/2} l_0$  and  $L_y = n_y \cdot 3 l_0 / 2$  are the lengths of the honeycomb in the  $x$  and  $y$  directions, respectively, with  $l_0$  denoting the cell-wall length of a full cell, and  $n_x$  and  $n_y$  being integers, as shown in Fig. 1(a). The relative density of a honeycomb is specified by

$$\rho = \rho^* / \rho_s = \frac{1}{A} \sum h_q l_q \tag{1}$$

where  $\rho^*$  is the density of honeycomb,  $\rho_s$  the density of its cell-wall material,  $l_q$  the  $q$ -th cell-wall length and  $h_q$  the corresponding thickness. The cell walls near the boundary of the area  $A_0$  are of the length of  $l_0/2$ . For the basic topology model, each full cell has six equal walls but every two neighboring cells share one wall, so the total length of all cell-walls in the area  $A_0$  is  $3Nl_0$  with  $N = n_x \cdot n_y$ . The cell-wall thickness is identical and it can be calculated by

$$h_0 = \rho A_0 / 3Nl_0 = \sqrt{3} \rho l_0 / 2 \tag{2}$$

Three types of microstructural randomness and imperfections, i. e., randomly removing cell walls, randomly thickening cell walls, and cell irregularity, are employed in the basic topology model. For simplicity, the honeycomb (HC) models are denoted as

- HC-0: Regular honeycomb;
- HC-1: Regular honeycomb with randomly removing cell walls;
- HC-2: Regular honeycomb with randomly thickening cell walls;
- HC-3: Irregular honeycomb.

The details of the corresponding technique are described as follows.

The HC-1 model is characterized by a removing ratio,  $k_1$ , defined as

$$k_1 = N_1 l_0 / 3Nl_0 = N_1 / 3N \tag{3}$$

where  $N_1$  is the number of removing cell walls, and only the cell walls with full length  $l_0$  are considered to randomly remove. For a given relative density, the cell-wall thickness of HC-1 is

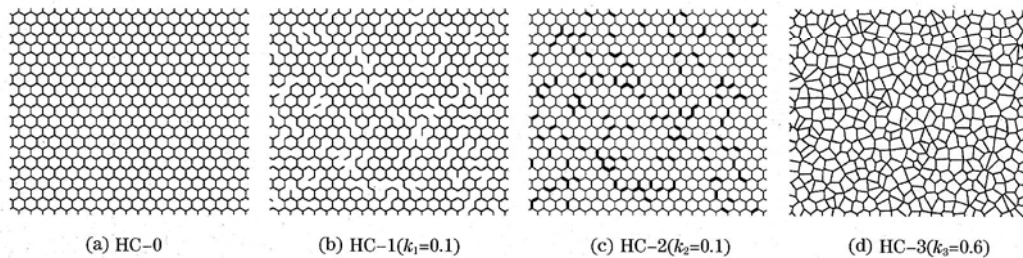


Fig. 1. Regular hexagonal honeycomb and honeycombs with microstructural randomness and imperfections.

revised as

$$h_1 = \rho A_0 / (3Nl_0 - N_1 l_0) = h_0 / (1 - k_1) \quad (4)$$

The HC-2 model is characterized by a thickening ratio,  $k_2$ , defined as,

$$k_2 = N_2 l_0 / 3Nl_0 = N_2 / 3N \quad (5)$$

where  $N_2$  is the number of thickening cell walls, and only the cell walls with full length  $l_0$  are considered to randomly thicken. The thickness of the thickening cell-walls is twice that of the other cell-walls. For a given relative density, the cell-wall thickness of HC-1 is revised as

$$h_2 = \rho A_0 / (3Nl_0 + N_2 l_0) = h_0 / (1 + k_2) \quad (6)$$

The HC-3 model can be constructed by several methods and different methods may obtain different ranges of the cell irregularity. In the previous research<sup>[3]</sup>, we have employed two methods: the disorder of nodal locations of a regular honeycomb and the random generation of the nuclei's locations. The degree of cell irregularity in the honeycombs constructed by the first method is small and that produced by the second method is large. Another method by randomly disordering nuclei's locations used by Li et al.<sup>[14]</sup> can vary the cell irregularity in a much larger range, so it is employed here. The two-dimensional Voronoi technique contains the followings steps. Firstly,  $N$  nuclei are generated in the area  $A_0$  by regularly packing their positions as

$$\begin{cases} x_{0,ij} = [i - 1/2 + (-1)^j / 4] \cdot \sqrt{3} l_0 \\ y_{0,ij} = (j - 1) \cdot 1.5 l_0 \end{cases} \quad (7)$$

where  $3^{1/2} l_0$  is the distance of most neighboring nuclei,  $i = 1, \dots, n_x$  and  $j = 1, \dots, n_y$ . Secondly, each nucleus is randomly perturbed from its regularly packed location  $(x_{0,ij}, y_{0,ij})$ , so its coordinates  $(x_{ij}, y_{ij})$  are written as

$$\begin{cases} x_{ij} = x_{0,ij} + k_3 \sqrt{3} l_0 \cdot \alpha_{ij} \cos 2\pi\beta_{ij} \\ y_{ij} = y_{0,ij} + k_3 \sqrt{3} l_0 \cdot \alpha_{ij} \sin 2\pi\beta_{ij} \end{cases} \quad (8)$$

where  $\alpha_{ij}$  and  $\beta_{ij}$  are random numbers uniformly distributed between 0 to 1,  $k_3$  is a constant described the degree of cell irregularity. Thirdly, the nuclei are copied to the eight surrounding neighboring areas by translation. And then the set of these  $9N$  nuclei are used to construct the Delaunay triangulation and the Voronoi diagram. Finally, the Voronoi diagram in the area  $A_0$  is reserved to form the desired honeycomb. For a given relative density, the cell-wall thickness is calculated by

$$h_3 = \rho A_0 / \sum l_q \quad (9)$$

In this paper, the HC-0 model is constructed in an area of 103.92 mm × 90 mm with 400 nuclei ( $n_x = 20$  and  $n_y = 20$ ), as shown in Fig. 1(a), in which the length of cell-wall,  $l_0$ , is 3 mm. Samples with  $k_1 = 0.1$ ,  $k_2 = 0.1$  and  $k_3 = 0.6$  for the HC-1, HC-2 and HC-3 models, respectively, are shown also in Fig. 1. The zero value of  $k_i$  ( $i = 1, 2, 3$ ) corresponds to the HC-0 model. For each nonzero value of  $k_i$ , five samples are considered to study the statistical behavior. One value of relative density, i. e., 0.1, is specified for the four types of honeycombs. Another two values of relative density, i. e., 0.05 and 0.15, will also be considered for the HC-3 model later.

## 2.2. Finite Element Analysis

The in-plane crushing behavior of honeycombs under different impact velocity was investigated by finite element method using the ABAQUS/Explicit code. The specimen is sandwiched between two rigid platens and its contact edges can slip on both interfaces with slight friction. The friction coefficient is assumed to be 0.02. The cell walls of specimen are modeled with shell elements of type S4R (a 4-node quadrilateral shell element with reduced integration) with five integration points. For a regular honeycomb, each edge of the cell wall contains six elements. For an irregular honeycomb, the element number depends on the length of the cell wall. The average element length is about 0.5 mm. Cell walls shorter than the thickness were eliminated to speed up the calculation<sup>[3,14,15]</sup>. Each model consists of about 7500 shell elements. The length of specimen in the out-of-plane direction,  $L_z$ , is 1mm. The nodes in the front and back planes were limited to moving in the corresponding planes, and each node in the back plane was limited to synchronously moving with the mirror node in the front plane by the \* EQUATION command. Surface contact is specified between all faces of cells that may contact during crushing.

Three kinds of cell-wall materials were considered<sup>[1]</sup>. The first one is elastic-perfectly plastic with Young's modulus, yield stress and Poisson's ratio being 66 GPa, 175 MPa and 0.3, respectively. This material will be used everywhere except when specially notified. The other two materials are elastic-plastic with linear strain-hardening and elastic-perfectly plastic with strain-rate hardening. The stress-strain relations in the plastic stage for the last two materials are defined as

$$\sigma = \sigma_y + B\epsilon_p \quad (10)$$

and

$$\sigma = \sigma_y [1 + C \ln(\dot{\epsilon}_p / \dot{\epsilon}_0)] \quad (11)$$

respectively, where  $\epsilon_p$  is the equivalent plastic strain,  $\sigma_y$  the yield strength of cell-wall material,  $\dot{\epsilon}_p / \dot{\epsilon}_0$  the relative equivalent strain rate,  $B$  and  $C$  are material constants<sup>[16]</sup>. Here we take  $B = 175$  MPa and  $\dot{\epsilon}_0 = 0.1$ /s. Two levels of the strain-rate sensitivity with  $C = 0.05$  and  $C = 0.5$  are considered, which will be referred to Rate Sensitivity materials 1 and 2 (denoted as RS1 and RS2), respectively.

The uniaxial crushing is executed in the  $x$  and  $y$  directions. Specimens are laid on a stationary rigid platen and compressed by another rigid platen with a constant velocity  $V_0$ . The compression force, stress, displacement and strain are taken to be positive. The nominal strain and strain-rate are defined to reflect the averaged deformation and deformation rate, respectively, but they are only for the purpose of comparison, because when the global deformation localization takes place these definitions will lose their physical meaning. For the purpose of quantitative comparison and analysis, the plateau stress is defined as

$$\sigma_{pl} = \frac{1}{\epsilon_D - \epsilon_y} \int_{\epsilon_y}^{\epsilon_D} \sigma(\epsilon) d\epsilon \quad (12)$$

where  $\epsilon_y$  is the yield strain and  $\epsilon_D$  is the densification strain. The densification strain was determined by calculating the maximum of the efficiency of energy absorption<sup>[17,18]</sup>

$$\eta(\epsilon) = \frac{1}{\sigma(\epsilon)} \int_0^{\epsilon} \sigma(\epsilon) d\epsilon \quad (13)$$

### III. MICROSTRUCTURAL EFFECTS ON THE DYNAMIC MECHANICAL PROPERTIES

#### 3.1. Deformation Modes and Critical Impact Velocities

For the in-plate crushing of regular honeycombs, three deformation patterns ("X", "V" and "I"-shaped patterns) corresponding to different impact velocities have been reported<sup>[19]</sup>. Besides the "X"-shaped pattern, different patterns also can be found at a low impact velocity, since the crushing bands are induced by the weakest links in a fairly homogeneous stress field and their location is highly sensitive to the details of boundary conditions as well as the height-to-width ratio of specimen<sup>[3]</sup>. However, with the increase of the impact velocity, the inertia effect will dominate the deformation and lead to the deformation localization at the impact end.

For the in-plate crushing of imperfect honeycombs, more complicated deformation patterns have been observed due to the new competitive mechanism pertinent to the microstructural randomness and imperfections<sup>[3-5]</sup>. The macroscopic deformation for the irregular honeycombs was categorized into three modes according to the impact velocity<sup>[3]</sup>. At a low impact velocity, a Quasi-static Mode with multiple randomly distributed crush bands occurs, while at a very high impact velocity, a Dynamic Mode with a progressive layer by layer collapse band forms from the impact end. A *Transitional Mode* occurs at a moderate impact velocity, in which crush bands are concentrated near the impact end. For the Quasi-static Mode, the stress waves reflect back and forth through the specimen for several times and so the stress is macroscopically homogeneous, but for the Dynamic Mode, the deformation occurs like a manner of shock wave propagating through the cellular materials. Due to these understanding, these two modes were also named respectively as the *Homogeneous Mode* and the *Shock Mode*<sup>[6]</sup>, which will be inherited in this paper. Other optional names, such as the random mode and the progressive mode, have been used in the literature [2].

Deformation patterns at a nominal strain of 0.6 of regular and imperfect honeycombs crushed in the  $x_1$  direction at different impact velocities are shown in Fig. 2. Deformation mode maps for

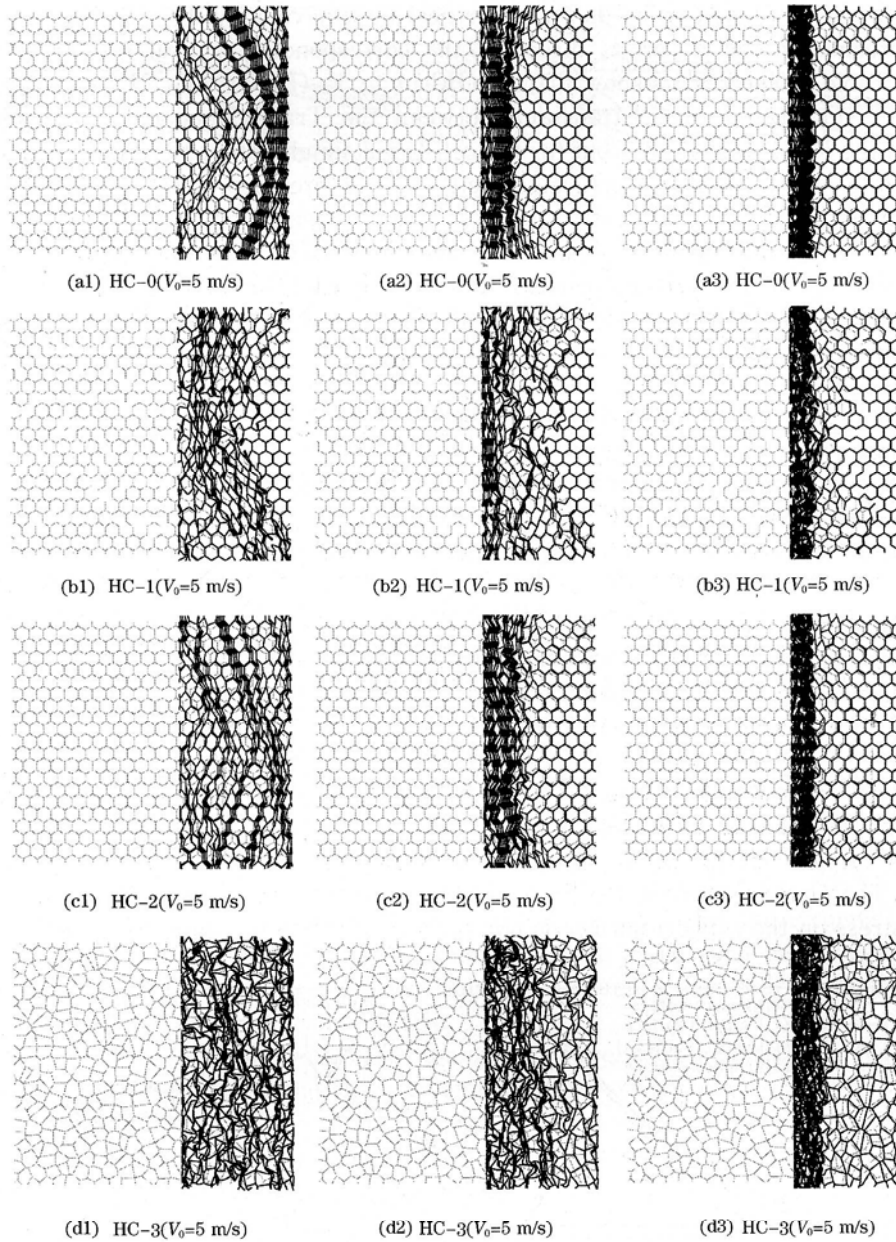


Fig. 2. Deformation patterns of honeycombs crushed in the  $x_1$  direction at different impact velocities with the nominal strain of 0.6.

honeycombs can be constructed through the empirical observation<sup>[3]</sup>, but the quantitative critical impact velocities for modes transition are not easy to obtain. To determine the critical impact velocity for mode transition between the Quasi-static and Transitional modes  $V_{cl}$ , Liu et al. <sup>[1]</sup> proposed a uniformity coefficient of plateau stress, here named as Stress Uniformity Index (SUI), which is defined as

$$SUI = \sigma_{pl}^s / \sigma_{pl}^i \quad (14)$$

where  $\sigma_{pl}^i$  and  $\sigma_{pl}^s$  are the plateau stresses on the impact and support surfaces, respectively. The variations of the SUI with impact velocity for the regular and imperfect honeycombs are shown in Fig. 3. If the

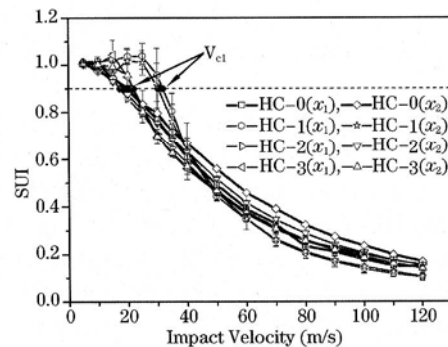


Fig. 3. Variation of the Stress Uniformity Index (SUI) with impact velocity.

critical value of SUI is taken to be 90%, the critical impact velocity  $V_{cl}$  can be calculated. For a honeycomb crushed in the  $x_1$  or  $x_2$  direction, the corresponding critical impact velocity  $V_{cl}$  is presented in Table 1. The results show that  $V_{cl}(HC-1) > V_{cl}(HC-3) > V_{cl}(HC-0) > V_{cl}(HC-2)$ . The critical impact velocity for mode transition between the Transitional and Shock modes  $V_{c2}$  is considered in the R-P-P-L model<sup>[20]</sup>, but for the cell-based simulation or the experiment, it is hard to give an accurate definition of the critical velocity. In our previous work, this critical velocity is determined by observing the deformation process. When the honeycomb is collapsed layer by layer, the honeycomb is regarded as deforming in the Shock Mode. The minimum impact velocity for this mode is taken as the critical velocity of mode transition. For all these honeycombs in this paper, the critical velocity  $V_{c2}$  is found to be about 80 m/s. The accurate definition of this critical velocity is open and desired.

Table 1. Critical impact velocity,  $V_{cl}$ .

$V_{cl}$ (m/s)	HC-0	HC-1	HC-2	HC-3
Crushed in the $x_1$ direction	20.1	31.9	17.4	22.0
Crushed in the $x_2$ direction	19.4	30.4	17.8	21.9

### 3.2. Plateau Stress

For cellular materials under crushing, the nominal stress-strain curve exhibits three regions, i. e. elastic region, stress plateau region and densification region. In the stress plateau region, the stress keeps at an almost constant level within a large strain range. Hence, the plateau stress has been used as the most important property to characterize the dynamic response of cellular materials. For a series of impact velocities, the plateau stresses on the impact and support surfaces are calculated. The plateau stress of the HC-0 model is shown in Fig. 4 (a). Uniaxial dynamic crushing was carried out in the  $x_1$  and  $x_2$  directions. Anisotropy response is found in regular honeycombs. The plateau stress on the impact surface heavily dependent on the impact velocity, but the plateau stress on the support surface is not very sensitive to the impact velocity.

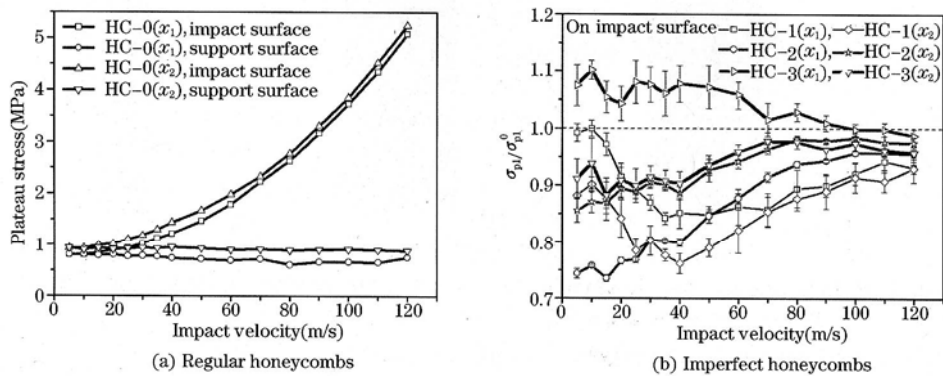


Fig. 4. Plateau stresses of regular honeycombs and relative plateau stresses of imperfect honeycombs.

Three types of microstructural randomness and imperfections have been used in our numerical simulations. The corresponding plateau stresses are also calculated. Here, we only consider the plateau stress on the impact surface. The plateau stresses of HC-1 with  $k_1 = 0.1$ , HC-2 with  $k_2 = 0.1$  and HC-3 with  $k_3 = 0.6$  on the impact surface are calculated for different impact velocities, and compared with those of HC-0 in Fig. 4 (b). The results show that almost all these types of microstructural randomness and imperfections lead to a decrease in the plateau stress. For the HC-1 model, the weakening effect is especially obvious at a moderate impact velocity, i. e. when the transitional mode occurs. For the HC-2 model, the weakening effect is particularly severe at a low impact velocity, but with the increase of the impact velocity, this effect almost disappears. Similar

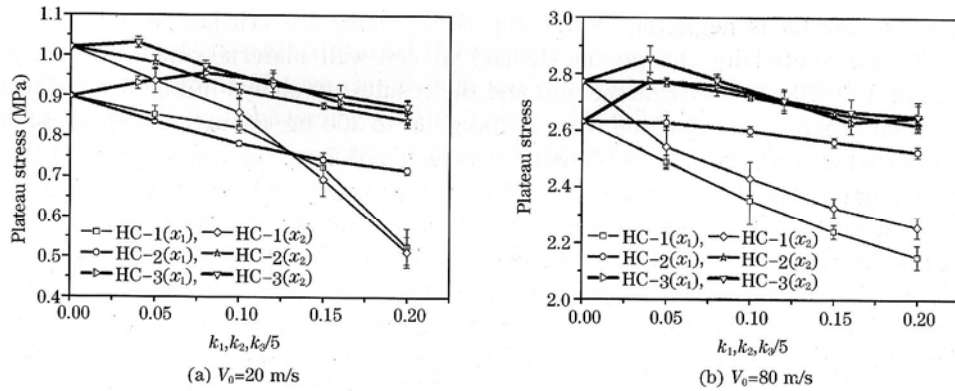


Fig. 5. Variations of plateau stress on the impact surface with the imperfect microstructural parameters.

behavior is found for the HC-3 model crushing in the  $x_2$  direction. However, for the HC-3 model crushing in the  $x_1$  direction, an enhancing effect is found at a not very high impact velocity. It implies that increasing the irregularity may help to improve the energy absorption capacity, but it depends on the crushing direction and impact velocity.

For two specific impact velocities, variations of plateau stress on the impact surface with the imperfect microstructural parameters are shown in Fig. 5. It should be noted that the imperfect microstructural parameters,  $k_1$ ,  $k_2$  and  $k_3$ , are not comparable. Curves with different imperfect microstructural parameters plotted in the same figure are just for convenience. It is found that increasing the removing ratio leads to a decrease in the plateau stress. However, as the cell irregularity increases, the plateau stress first increases and then decreases. Increasing cell irregularity eliminates the anisotropy behavior.

#### IV. POSSIBLE MECHANISMS GOVERNING THE RATE SENSITIVITY

In this section, the HC-3 model with  $k_3 = 0.6$  (i. e., Voronoi honeycombs) is employed. Crushing in the  $x_1$  direction is considered. Influences of the inertia and the properties of cell-wall materials on the dynamic response of Voronoi honeycombs under impact are investigated.

##### 4.1. Influence of Inertia and Micro-inertia

A numerical ‘test’ method by changing the density of cell-wall material was developed by Yu et al. [6,1]. This method provides the most straightforward evidence for the inertia effect. Much previous work has shown that the plateau stress on the impact surface varies squarely with the impact velocity<sup>[19,20]</sup>. Our results further indicate the physical mechanism is the inertia effect. When the honeycombs are crushed in Homogeneous Mode, the nominal stress-strain curves under different impact velocities remain almost identical, regardless of different densities of cell-wall material, as shown in Fig. 6(a). This implies that, when the deformations of the honeycombs are macroscopically

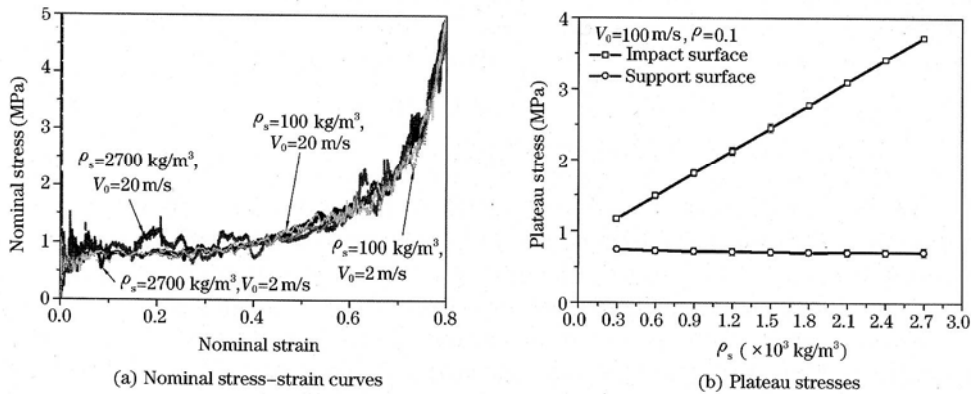


Fig. 6. Variations of nominal stress-strain curves and plateau stresses with the density of cell-wall material.

homogeneous, the inertia is negligible. When the honeycombs are crushed at a moderate or high impact velocity, we artificially change the density of cell-wall material and evaluate the plateau stress. A case of  $V_0 = 100$  m/s was carried out and the results are shown in Fig. 6(b). The density of cell-wall material is artificially changed from  $2700 \text{ kg/m}^3$  to  $300 \text{ kg/m}^3$  with a step of  $-300 \text{ kg/m}^3$ , but the microstructure and the relative density of honeycomb keep unchanged. For all these cases, the honeycombs deform in the shock or transitional mode. The plateau stress on the impact surface keeps almost constant. This implies the plateau stress on the support surface is independent with the density of cell-wall material. But it depends on the relative density of sample as indicated in the previous section. A linear variation of the plateau stress on the impact surface with the density of cell-wall material is found. With the reduction of the density of cell-wall material, the plateau stresses on the impact and support surfaces become close, which implies the force equilibrium and uniform deformation become much easier<sup>[1]</sup>. So the inertia effect plays a significant role in the dynamic crushing of honeycombs.

Extensive investigations have shown that the inertia plays a very important role in the dynamic crushing of cellular materials, which may lead to the deformation localization due to their high porosity. The inertia of the material leads to the macroscopic deformation localization and stress nonuniformity. Changing the relative density of honeycomb by changing the thickness of cells leads to different dynamic response, as shown in Fig. 7(a). It can be seen that the plateau stresses on the impact and support surfaces increase with increasing relative density of honeycomb for all impact velocities. A rapid increase of plateau stress on the impact surface with the increasing impact velocity can be found for the cases of high relative density of honeycomb. This presents an evidence of the inertia effect.

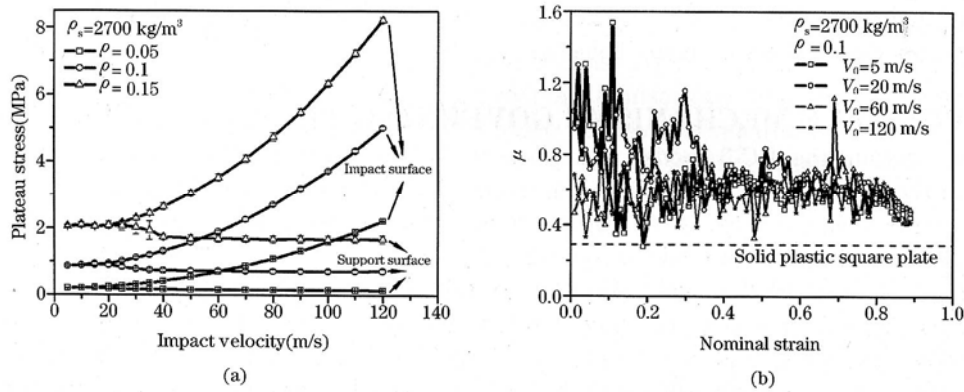


Fig. 7. (a) Variation of plateau stress with impact velocity for honeycombs with different relative densities; (b) Comparison of the transverse-to-longitudinal acceleration ratio under different impact velocities.

Micro-inertia effect was frequently used to qualitatively explain the significant elevation of collapse stress in the dynamic response of cellular materials<sup>[22-24]</sup>, but quantitative work is less. A proposal was suggested by Liu et al.<sup>[1]</sup>, who introduced a transverse-to-longitudinal acceleration ratio, defined as

$$\mu = \sqrt{\frac{1}{n} \sum_{i=1}^n a_{y,i}^2} / \sqrt{\frac{1}{n} \sum_{i=1}^n a_{x,i}^2} \quad (15)$$

where  $a_{x,i}$  and  $a_{y,i}$  are the node accelerations of finite element mesh,  $n$  is the node number. For cellular materials, this ratio can characterize both the macroscopic and microscopic transverse inertia effects. For four cases of impact velocities, this ratio is calculated and shown in Fig. 7(b), in which the density of cell-wall material is  $2700 \text{ kg/m}^3$ , the relative density of honeycomb is 0.1, and only the first sample of HC-3 ( $k_3 = 0.6$ ) was considered. The results show that the ratio is about 0.6, which is larger than that of a solid plastic square plate ( $\mu = vL_x/2L_y = 0.29$ , where  $v = 0.5$ ) but much smaller than that of a typical Type II structure<sup>[1]</sup>. Hence, the micro-inertia effect in irregular Voronoi honeycombs is relatively weak. It can also be noticed that the value of the ratio  $\mu$



decreases with increasing impact velocity.

#### 4.2. Influence of the Cell-wall Material Properties

In the numerical simulation, we can change the cell-wall material properties to investigate its influence on the crushing behavior<sup>[6,1]</sup>. The linear strain-hardening and strain-rate hardening elastic-plastic materials have been selected to study the dynamic responses of honeycombs under various impact velocities. The plateau stresses on the impact and support surfaces of Voronoi honeycombs made of different cell wall materials under different impact velocities are calculated and shown in Fig. 8(a). The results show that the strain hardening and strain-rate hardening lead to an increase in the plateau stress. The most significant increase in the plateau stress compared to that of the rate independent, elastic-perfectly plastic material is that of material RS2.

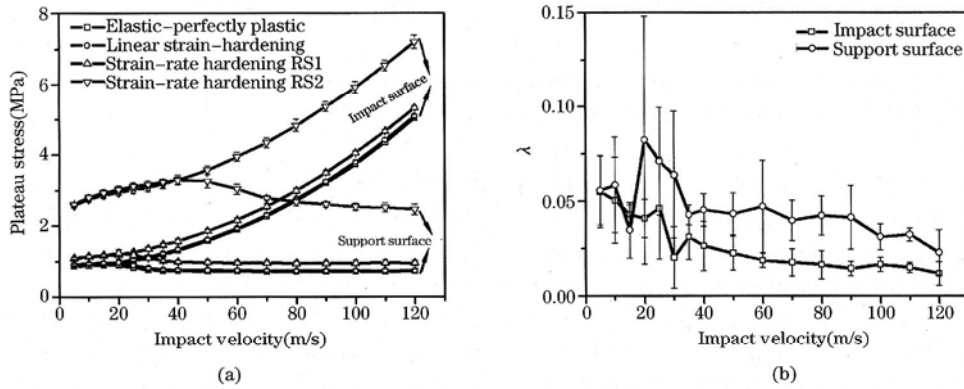


Fig. 8. (a) Comparison of the plateau stresses on the impact and support surfaces of Voronoi honeycombs made of different cell wall materials under different impact velocities; (b) Relative increase in the plateau stress of honeycombs made of strain-hardening material under different impact velocities.

To evaluate the increase of the plateau stress due to strain hardening, a parameter  $\lambda$  was defined as<sup>[6,1]</sup>

$$\lambda = (\sigma_{pl}^{SH} - \sigma_{pl}^{EPP}) / \sigma_{pl}^{EPP} \quad (16)$$

where  $\sigma_{pl}^{EPP}$  and  $\sigma_{pl}^{SH}$  are the plateau stresses of the elastic-perfectly plastic material and the strain-hardening material, respectively. The relative increases in the plateau stresses on the impact and support surfaces are calculated and shown in Fig. 8(b). It shows that  $\lambda$  keeps small over the whole range of the impact velocities studied. Hence, the strain-hardening of cell-wall material has minor influence on the quasi-static and dynamic responses of honeycombs.

Similarly, to evaluate the increase of the plateau stress due to the strain-rate hardening, a parameter  $\eta_1$  was defined as<sup>[6,1]</sup>

$$\eta_1 = (\sigma_{pl}^{RSH} - \sigma_{pl}^{EPP}) / \sigma_{pl}^{EPP} \quad (17)$$

where  $\sigma_{pl}^{RSH}$  is the plateau stress of honeycombs made of the strain-rate hardening material. According to Eq. (11), the relative increase in the flow stress of cell-wall material is described by

$$\eta_2 = (\sigma - \sigma_y) / \sigma_y = C \ln(\dot{\epsilon}_p / \dot{\epsilon}_0) \quad (18)$$

The variation of the relative increase in the plateau stress with the nominal strain-rates for honeycombs made of materials RS1 and RS2 is shown in Fig. 9. The relative increase in the plateau stress on the impact surface is always less than the relative increase in the flow stress of the cell-wall material. But, for material RS1, when the strain-rate is about 250/s, the relative increase in the plateau stress on the support surface can be larger than the relative increase in the flow stress of the cell-wall material. The relative increase in the plateau stress due to the strain-rate sensitivity of cell-wall material becomes small when the strain-rate is very high. The results show that for cell-wall materials with high strain-rate sensitivity, the increase in plateau stress can be much large. From the data on the impact surface, when the honeycomb is deformed in the Transitional Mode or the Shock Mode, the strain-rate effect decreases rapidly but the inertia effect increases fast with increasing impact velocity.

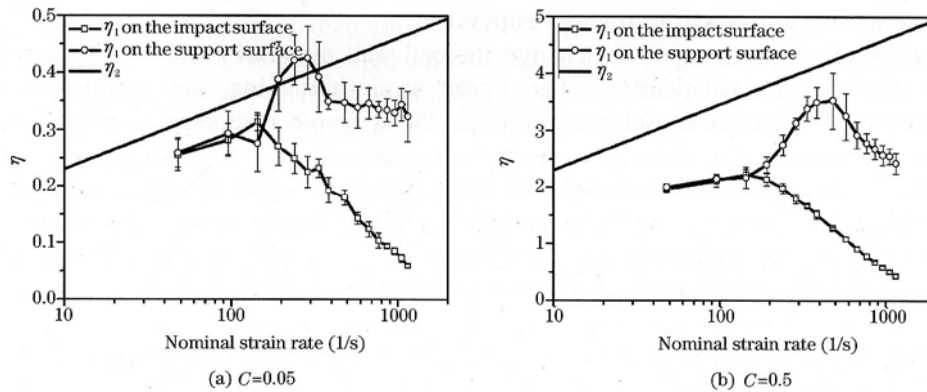


Fig. 9. Relative increase in plateau stress of honeycombs made of strain-rate hardening materials at different nominal strain-rates.

## V. CONCLUSIONS

Three types of microstructural randomness and imperfections, i. e. , randomly removing cell walls, randomly distributed solid inclusions, and cell irregularity, were employed in the basic topology model of a regular hexagonal honeycomb. Their influences on deformation mode and plateau stress were studied by finite element method using the ABAQUS/Explicit code. Three macroscopic deformation modes occur when a honeycomb is compressed under different impact velocities. At a low impact velocity, a Quasi-static Mode with multiple randomly distributed crush bands occurs, while at a very high impact velocity, a Shock Mode with a progressive layer by layer collapse band forms from the impact end. A Transitional Mode occurs at a moderate impact velocity, in which the crush bands are concentrated near the impact end. Statistical results show that microstructural randomness and imperfections may strongly affect the energy absorption capacity.

The influences of the inertia and the properties of cell-wall materials on the rate sensitivity of Voronoi honeycombs were explored with numerical ‘test’ methods. The density of cell-wall material was artificially changed to study the influence of inertia, which was found to be the dominant factor in the dynamic crushing of Voronoi honeycombs. The inertia of the material leads to the macroscopic deformation localization and stress nonuniformity, and so the nominal stress-strain curve loses its physical meaning. The effects of strain hardening and strain-rate hardening of cell-wall materials were explored, but it was found that they result to a slight increase in plateau stress, which cannot explain the strong rate dependence observed in some metal foams. Some other possible mechanisms (e. g. ductile-brittle transition of the cell-wall material, strain-rate sensitivity of its failure strain) responsible to the rate sensitivity of honeycombs need to be further investigated.

## References

- [1] Liu, Y. D. , Yu, J. L. , Zheng, Z. J. and Li, J. R. , A numerical study on the rate sensitivity of cellular metals. *International Journal of Solids Structures*, 2009, 46(22-23) : 3988-3998.
- [2] Ma, G. W. , Ye, Z. Q. and Shao, Z. S. , Modeling loading rate effect on crushing stress of metallic cellular materials. *International Journal of Impact Engineering*, 2009, 36(6) : 775-782.
- [3] Zheng, Z. J. , Yu, J. L. and Li, J. R. , Dynamic crushing of 2D cellular structures: A finite element study. *International Journal of Impact Engineering*, 2005, 32(1-4) : 650-664.
- [4] Kou, D. P. , Effects of meso-structure on the mechanical behavior and multi-objective optimization design of cellular metals. Dissertation. University of Science and Technology of China, 2008 (in Chinese).
- [5] Kou, D. P. , Yu, J. L. and Zheng, Z. J. , Effect of randomly removing cell walls on the dynamic crushing behaviour of honeycomb structures. *Lixue Xuebao/Chinese Journal of Theoretical and Applied Mechanics*, 2009, 41(6) : 859-868 (in Chinese).
- [6] Yu, J. L. , Liu, Y. D. , Zheng, Z. J. , Li, J. R. and Yu, T. X. , Influences of inertia and material

- property on the dynamic behavior of cellular metals. IUTAM Symposium on Mechanical Properties of Cellular Materials (September 17-20, 2007, LMT-Cachan, Cachan, France), eds H. Zhao and N. A. Fleck, Springer, pp. 149-157.
- [7] Liu, Y. D. , Yu, J. L. and Zheng, Z. J. , Effect of inertia on the dynamic behavior of cellular metal. *Gaoya Wuli Xuebao/Chinese Journal of High Pressure Physics*, 2008, 22(2) : 118-124 (in Chinese).
- [8] Liu, Y. D. , Numerical analysis of the rate effect and theoretical study on the dynamic behavior of cellular metals. Dissertation. University of Science and Technology of China, 2010(in Chinese).
- [9] Chen, C. , Lu, T. J. and Fleck, N. A. , Effect of imperfections on the yielding of two dimensional foams. *The Journal of Mechanics and Physics of Solids*, 1999, 47(11) : 2235-2272.
- [10] Nakamoto, H. , Adachi, T. and Araki, W. , In-plane impact behavior of honeycomb structures randomly filled with rigid inclusions. *International Journal of Impact Engineering*, 2009, 36(1) : 73-80.
- [11] Nakamoto, H. , Adachi, T. and Araki, W. , In-plane impact behavior of honeycomb structures filled with linearly arranged inclusions. *International Journal of Impact Engineering*, 2009, 36(8) : 1019-1026.
- [12] Liu, Y. and Zhang, X. C. , The influence of cell micro-topology on the in-plane dynamic crushing of honeycombs. *International Journal of Impact Engineering*, 2009, 36(1) : 98-109.
- [13] Qiu, X. M. , Zhang, J. and Yu, T. X. , Collapse of periodic planar lattices under uniaxial compression, part II: Dynamic crushing based on finite element simulation. *International Journal of Impact Engineering*, 2009, 36(10-11) : 1231-1241.
- [14] Li, K. , Gao, X. L. and Wang, J. , Dynamic crushing behavior of honeycomb structures with irregular cell shapes and non-uniform cell wall thickness. *International Journal of Solids and Structures*, 2007, 44(14-15) : 5003-5026.
- [15] Schaffner, G. , Guo, X. D. E. , Silva, M. J. and Gibson, L. J. , Modelling fatigue damage accumulation in two-dimensional Voronoi honeycombs. *International Journal of Mechanical Science*, 2000, 42(4) : 645-656.
- [16] Johnson, G. R. and Cook, W. H. , A constitutive model and data for metals subjected to large strains, high strain rates and high temperatures. In: *Proceedings of the Seventh International Symposium on Ballistics*, The Hague, Netherlands, 1983, pp. 541-547.
- [17] Avallè, M. , Belingardi, G. and Montanini, R. , Characterization of polymeric structural foams under compressive impact loading by means of energy-absorption diagram. *International Journal of Impact Engineering*, 2001, 25(5) : 455-472.
- [18] Tan, P. J. , Reid, S. R. , Harrigan, J. J. , Zou, Z. and Li, S. , Dynamic compressive strength properties of aluminium foams. Part I — experimental data and observations. *The Journal of Mechanics and Physics of Solids*, 2005, 53(10) : 2174-2205.
- [19] Ruan, D. , Lu, G. , Wang, B. and Yu, T. X. , In-plane dynamic crushing of honeycombs—a finite element study. *International Journal of Impact Engineering*, 2003, 28(2) : 161-182.
- [20] Tan, P. J. , Reid, S. R. , Harrigan, J. J. , Zou, Z. and Li, S. , Dynamic compressive strength properties of aluminium foams. Part II — ‘shock’ theory and comparison with experimental data and numerical models. *The Journal of Mechanics and Physics of Solids*, 2005, 53(10) : 2206-2230.
- [21] Li, Q. M. and Reid, S. R. , About one-dimensional shock propagation in a cellular material. *International Journal of Impact Engineering*, 2006, 32(11) : 1898-1906.
- [22] Su, X. Y. , Yu, T. X. and Reid, S. R. , Inertia-sensitive impact energy-absorbing structures. Part I: Effects of inertia and elasticity. *International Journal of Impact Engineering*, 1995, 16(4) : 651-672.
- [23] Su, X. Y. , Yu, T. X. and Reid, S. R. , Inertia-sensitive impact energy-absorbing structures. Part II: Effect of strain rate. *International Journal of Impact Engineering*, 1995, 16(4) : 673-689.
- [24] Reid, S. R. and Peng C. , Dynamic uniaxial crushing of wood. *International Journal of Impact Engineering*, 1997, 19(5-6) : 531-570.